ACCURACY ASSESSMENT TOWARD MERGING OF TERRESTRIAL LASER SCANNER POINT DATA AND UNMANNED AERIAL SYSTEM POINT DATA

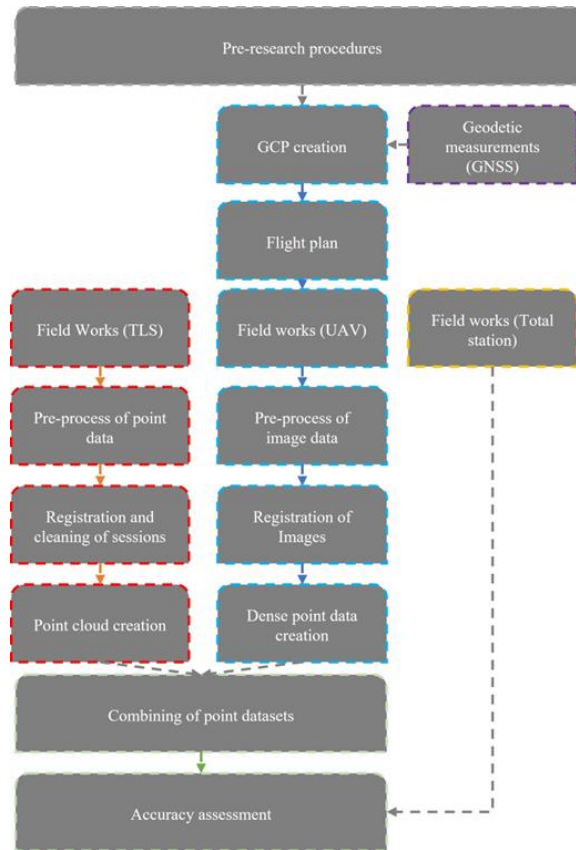**[1]Lütfiye KARASAKA** ⓘ **, [2*]Hasan Bilgehan MAKİNECİ** ⓘ **, [3]Kasım ERDAL** ⓘ

Konya Teknik Üniversitesi, Mühendislik ve Doğa Bilimleri Fakültesi, Harita Mühendisliği Bölümü, Konya, TÜRKİYE
[1]lkarasaka@ktun.edu.tr, [2]hbmakineci@ktun.edu.tr, [3]f218223001006@ktun.edu.tr

Highlights

- UAV and TLS point clouds can be integrated and the integration improves the understanding, interpretation and quality of data

- UAV is a complementary data source with insufficient data produced with TLS, likewise TLS is a complementary data source when the data created with UAv is inadequate

- Measurements with merged point clouds generate satisfactory metric results

Graphical Abstract

The workflow of the study

*Corresponding Author: Hasan Bilgehan MAKİNECİ, hbmakineci@ktun.edu.tr

ACCURACY ASSESSMENT TOWARD MERGING OF TERRESTRIAL LASER SCANNER POINT DATA AND UNMANNED AERIAL SYSTEM POINT DATA

[1]Lütfiye KARASAKA , **[2*]Hasan Bilgehan MAKİNECİ** , **[3]Kasım ERDAL**

Konya Teknik Üniversitesi, Mühendislik ve Doğa Bilimleri Fakültesi, Harita Mühendisliği Bölümü, Konya, TÜRKİYE
[1] lkarasaka@ktun.edu.tr, [2] hbmakineci@ktun.edu.tr, [3] f218223001006@ktun.edu.tr

ABSTRACT: Terrestrial Laser Scanning (TLS) techniques are widely preferred for 3D models of small and large objects, buildings, and historical and cultural heritages. However, sometimes relying on a single method for 3D modelling an object/structure is insufficient to arrive at a solution or meet expectations. For example, Unmanned Aerial Systems (UAS) provide perspective for building roofs, while terrestrial laser scanners provide general information about building facades. In this research, several facades of a selected building could not be modelled using terrestrial laser scanning, and UAS was used to complete the missing data for 3D modelling. The transformation matrix, a linear function, is created to merge different data types. In the transformation matrix, the scale was found to be 1:1.012. The accuracy analysis of the produced 3D model was also made by comparing the spatial measurements taken from different building facades and the differences in the measurement values obtained from the 3D model and calculating statistically. According to the accuracy analysis results, the Root Mean Square Error (RMSE) value is approximately 3 cm. The results of the accuracy research, which are within the 95% confidence interval with the three-sigma rule, are approximately 2 cm as RMSE. As a result of the study, it was determined that the data obtained from UAV photogrammetry and the data obtained by the TLS technique could be combined, and the integrated 3D model obtained can be used more efficiently.

Keywords: *Merging of Point Data, Terrestrial Laser Scanning, Unmanned Aerial Systems, 3D Modelling*

1. INTRODUCTION

3D modeling is the vectorial representation of the geometric information of an object in a computer environment. Today, 3D models of the physical earth or any object can be obtained by analyzing numerical data acquired using perspective imaging geometry and photogrammetric mathematical principles in a computer environment [1]. In addition, vectorial and visual presentations of the obtained 3D models can be made easily. Close-up photogrammetry and terrestrial laser scanning (TLS) are frequently preferred techniques for creating 3D models of small to large objects, buildings, and historical and cultural artifacts [2-4]. TLS has been a popular measurement technique in recent years for documenting objects, figures, historical buildings, and cultural heritages [5-7]. Point data produced by high-resolution laser scanning offers various solutions in cases where conventional techniques are impractical or impossible to apply [6, 8-10]. Unmanned Aerial Systems (UASs) are cost-effective systems capable of low-altitude flight, which can be operated remotely due to their pilotless use [10-12].

As a photogrammetry technique, image acquisition with UAS enables photogrammetric evaluation of the obtained images [13-14]. The evaluated data can then be used in various engineering projects, map production, documentation of historical/archaeological artifacts, and 3D modeling of objects and figures [15-16]. In addition, one significant feature is that the UAS collects data without endangering human life [17].

However, sometimes using a single method for 3D reconstruction of an object/structure may be

---

*Corresponding Author: Hasan Bilgehan MAKİNECİ, hbmakineci@ktun.edu.tr

insufficient to arrive at a solution or meet expectations. For instance, when constructing a 3D model of a building, building facades can be modeled using close-up photogrammetry or the TLS method [18]. In contrast, the necessary perspective for building roofs can be provided by the aerial photogrammetry method. In such cases, when a single method is insufficient for 3D modeling research, the problem must be solved by combining data obtained from different platforms and measurement methods [2, 19-23]. Recent studies show that neither data from UAV images nor data from TLS could create the desired 3D model of a building. To get more accurate 3D models, combined data has been used recently. Today, the UAS and TLS methods are used in conjunction for biomass prediction, the documentation of buildings, historical artifacts, and archaeological sites in engineering applications [24-29].

This study applied a combination of the TLS technique and UAS photogrammetry technique data to create a 3D model of Meliha Ercan Guest House located on the Selçuk University Campus. While TLS point data for the front and side facades of the building have suitable viewing angles, the back facade of the building is limited to a garden wall adjacent to heavily wooded land with a sloped topography and data acquisition conditions for laser scanning could not be provided. For this reason, the 3D modeling of the missing areas, or, the back facade and roof of the building, was completed by combining the point data obtained from the images through the UAS. The root mean square errors (RMSE) and standard deviations (StD) of point differences were calculated to assess their accuracy. Then, three sigma tests were performed, and the same calculations were repeated for the differences within the 95% confidence interval [30-31].

2. MATERIAL AND METHODS

Within the study's scope, it aims to create a 3D model of the Meliha Ercan Guest House located on the Selçuk University Campus. In order to create the desired 3D model, other techniques such as classical terrestrial photogrammetry and the TLS method cannot produce adequate data for the back facade of the building. UAS and TLS, alternative measurement and modeling techniques were combined. Thus, while developing the 3D model, the point data for the building's back façade and the roof that could not be obtained using TLS was completed using the point cloud data obtained through the UAS method. While combining UAV images, the software presents an algorithmic infrastructure called Structure from Motion (SfM). It is an algorithm that creates key points from images depending on the shooting distances (base length) between images (base length) and camera positions (angular positioning with the terrain) and then creates point data in images by combining the least faulty points that can be mapped in more than one image (they are called tie points). All point data obtained from all sessions were processed, registered, and cleaned to get the gridded point cloud with TLS in Faro Scene Software. As well as TLS field works done, UAV got images from an aerial position. Either TLS point data or UAV images were used for the study to create a more accurate 3D model of building together. The average grid spacing for the point cloud was about 2 cm. The workflow chart displaying the scope of the study is given in Figure 1.

2.1. Study Area

The study area is Meliha Ercan Guesthouse located on the Selcuk University Alaeddin Keykubat Campus, Selçuklu, Konya (38° 01' 07" N, 32° 30'28" E). The guesthouse, located in the northwest part of the campus area on the inner campus highway, makes a good subject for 3D reconstruction with general photogrammetric techniques due to its architecture. However, the back facade of the building does not provide adequate conditions for data collection using a single photogrammetric technique because the back facade is limited by a garden wall adjacent to sloping and densely forested topography. High garden walls and landscaping in front of the wall limit the distance at which photographs can be taken in suitable directions and angles for close-up photogrammetry. Therefore, it is an insufficient measuring distance for the TLS. In addition, the barn area, which is located very close to the building on the right back facade, is another restraining factor to terrestrial measurement methods.
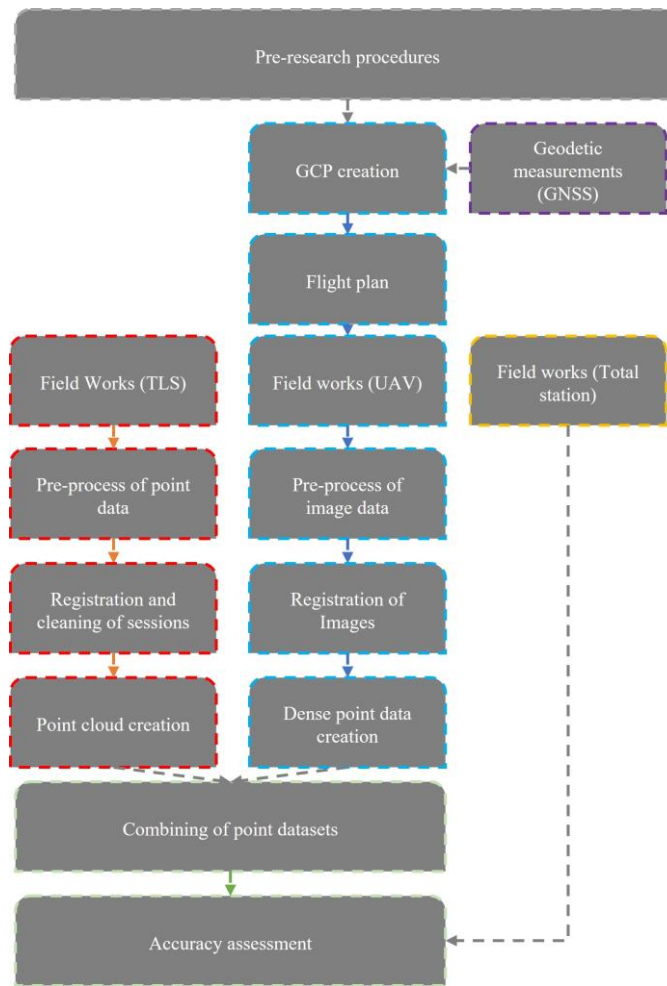
Figure 1. The workflow charts

Figure 2. The examples of problem definition of distances that restrict photogrammetric techniques between the building and the surrounding wall (A: Side Facade, B: Back Facade, C: Side Facade)

2.2. Data Acquiring

In this study, three different measurement systems were used to acquire the data.

◎   Total Station

As a classical measurement technique, data were collected from the area using a total station. Within this technique, a Sokkia Fx-101 total station (Figure 3A), which has a 1" angle measurement sensitivity, was applied. The manufacturer's default value for the distance measurement sensitivity is [(3+2 ppm x D) mm]. Without a reflector, the device can measure distances between 30 cm and 500 m using a laser with a battery life of approximately 20 hours.

◎   Faro Focus 3D X330

Faro Focus 3D X330 TLS produces realistic and detailed scanning results by scanning objects with a wide scanning range of up to 330 meters away with high precision and accuracy for detailed documentation and measurement. Laser technology is used to rapidly produce highly detailed 3D models of complex structures and objects. The distance between the laser scanner and the target is determined using the phase difference distance measurement method with the fixed infrared light waves reflected from the scanner [26] (Figure 3B).

◎   Parrot Anafi UAS

Parrot ANAFI features 180° integrated frame-based camera types that provide approximately 70° field of view and oblique image acquisition, as well as a camera resolution of 5472 × 3568 pixels, pixel size 2.41 × 2.41 µm, and a focal length of 8.8 mm. According to the General Directorate of Aviation of TURKEY UAS Regulations, it is a device under the toy class and does not require any legal license for use due to its weight of 320 g including the battery (Figure 3C).

Figure 3. Field researches (A: Terrestrial measurements made with the total station, B: Terrestrial measurements made with TLS, C: Measurement with UAS)

Within the scope of the research, the TLS was performed as the initial application. Prior to performing the TLS, the stations where the device will be placed were determined. Following that, target markings to

help register the scanning data were positioned around the building, and the front and side facades of the building were scanned with TLS. Each session lasted approximately 10 minutes, and each scan was overlapped by the previous scan. As a second method, UAS flights were carried out to obtain missing data for the back facade and roof of the building, which could not be scanned with TLS. In the study carried out to create the full 3D model of the object, the data obtained from the UAS method was used for the missing roof data and the back facade of the building that could not be scanned with the TLS method. Prior to the UAS flight, seven Ground Control Points (GCP) were established around the building, and their coordinates were obtained in real-time with the UTM projection CORS system. A flight plan was prepared using PIX4DCapture software to obtain aerial photographs of the building's roof and back facade for photogrammetric purposes in the UAS method. As a result, 114 images were obtained within the flight plan with a 1.51 cm/pix Ground Sampling Distance (GSD), and an 80% side and 70% forward overlap ratio. Parameters of the flight plans are given in Table 1.

In order to conduct accuracy analysis, measurements were taken from all facades of the building with the total station and compared with the length values obtained from the produced 3D model.

Table 1. Parameters of flight plan

Flight Parameters	Choice
Flight Height	52 m
GSD	1.51 cm/pix
Side overlap	80%
Forward overlap	70%
Image Number	114
Camera Angle	70
GCP Number	7
Flight Time (min.)	6.40

2.3. Data-Processing and Accuracy Assessment

Both closed source code commercial software and open-source code software were used to process and evaluate the data obtained from TLS and UAS measurements. To begin, the Scene software pre-processed and converted all the TLS raw data into a 3D point set shape. Following that, the merging of point clouds was manually combined using paper target marks homogeneously positioned on the building surfaces, as reflective target marks were not employed. Next, photogrammetric processes were performed using the Agisoft PhotoScan software, which uses Structure From Motion (SfM) based techniques [10, 30-32] (Deliry and Avdan 2021, Elkhrachy 2021, Jiménez-Jiménez, Ojeda-Bustamante et al. 2021, Xiao, Wang et al. 2021). Finally, TLS and UAS georeferenced point data were integrated with CloudCompare, an open-source code software, to produce a 3D structure model.

CloudCompare software enables various combining alternatives. This research integrated point data obtained from different sources with manual point selection (Figure 4). During manual point selection, TLS data is aligned with UAS data. In other words, the reference point dataset is the point data obtained from the UAS, and the target point data is data from the TLS scan (Figure 5A, Figure 5B). Thus, a 3D model was obtained by directly transforming the laser scanning data obtained in a local coordinate system into georeferenced UAS data (Figure 5C). Unnecessary points were removed from TLS and UAS data, resulting in the presentation of Figure 5D.
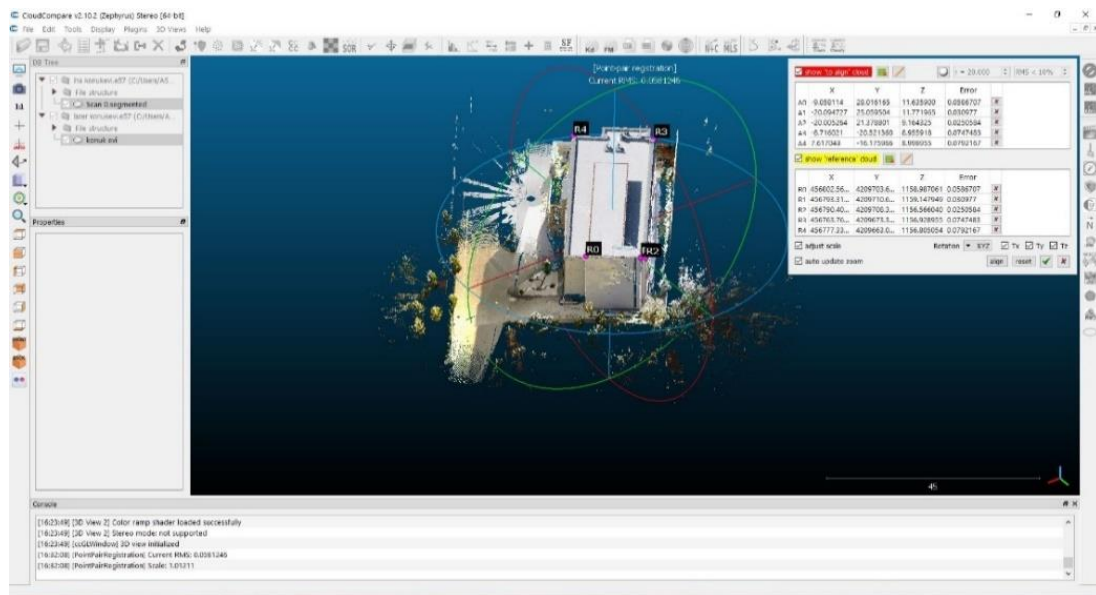
Figure 4. Integration of point data (manually combining of point data and transformation)
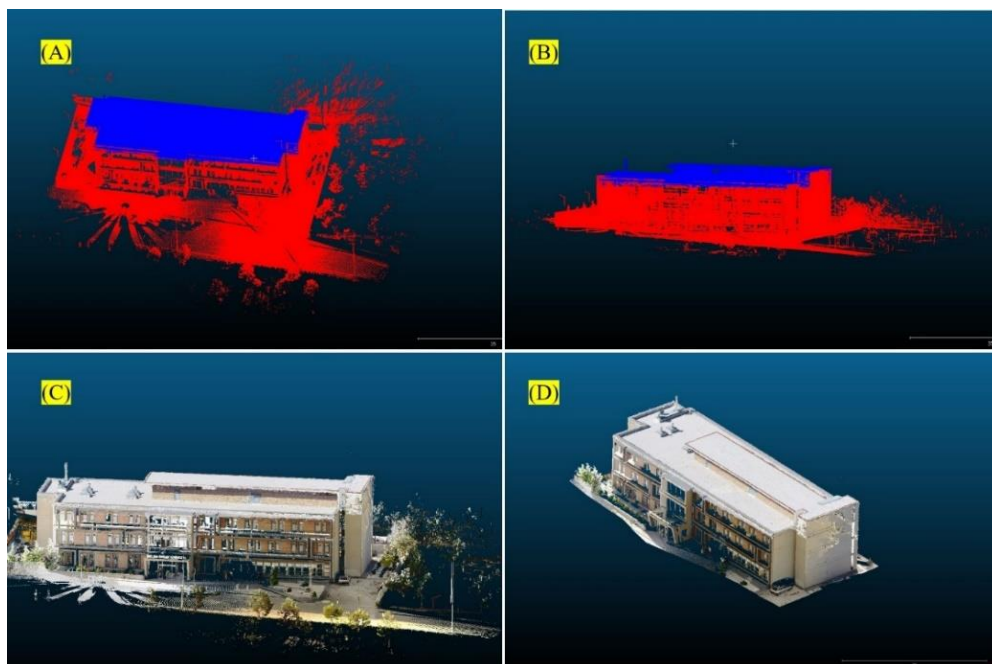

Figure 5. Integrated UAS and TLS point data (A and B: Dark blue UAS reference data and red TLS target data, C: Merged point data, D: Cleared merged point data)

3. RESULTS

The accuracy assessment of the 3D model, which is conducted through combining the point data obtained with TLS, an active detection method, with the point data obtained from the UAS camera images, a passive detection system, has been tested by investigating each facade of the building. This investigation was carried out by comparing measurements taken from all facades of the building at the field to those taken on the model. Figure 6 shows the sections on the building where the measurements taken with the total station are compared to the model measurements. Since there are two different data sources (UAV and TLS) in this research, a linear transformation matrix (a function) should be created between the different point data obtained from these two various data sources. As seen in Table 2, the RMSE value of

the obtained transformation matrix is approximately 6 cm. The scale was calculated as 1:1.012 on average.

Table 2. Parameters of transformation

RMSE	Scale	Transformation Matrix			
		A11	**A12**	**A13**	**A14**
		0.617	0.802	0.013	-14.506
		A21	**A22**	**A23**	**A24**
0.0581 m	1.0121	-0.802	0.617	0.005	-20.985
		A31	**A32**	**A33**	**A34**
		-0.004	-0.014	1.012	1147.526
		A41	**A42**	**A43**	**A44**
		0.000	0.000	0.000	1.000

In order to perform the accuracy analysis of the 3D model of the building, total station measurements were made, and the sizes of various details around the building were determined. With the 3D model, the actual dimensions of the building elements were listed, and the differences were calculated. Statistical analysis was carried out using the differences. RMSE and StD. values indicate that a high-accuracy 3D model has been produced. In Table 3, the measurements acquired on different building details on the front, back, and side facades and compares these with the measurements acquired on the model.
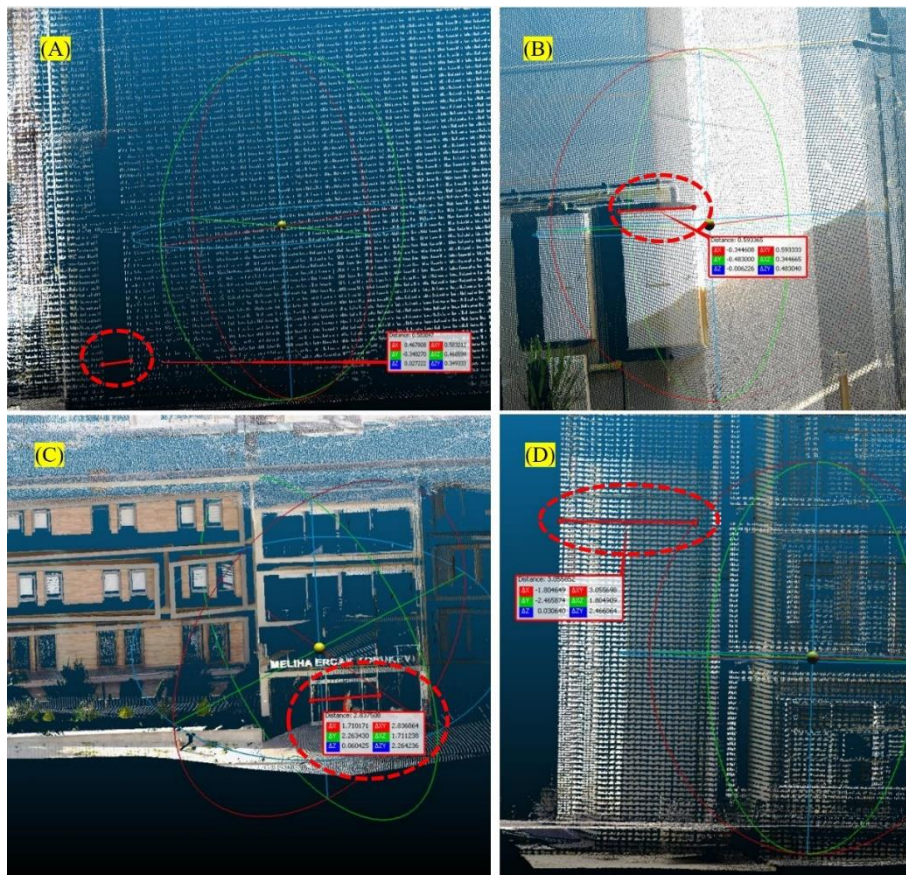
Figure 6. Comparison of the measurements (A: Measurement No 2, B: Measurement No 3, C: Measurement No 18, D: Measurement No 11)

Table 3. Comparison of the measurements

Facade	Measurement Number	Description	Measure from Field (m)	Measure from Model (m)	Differences (m)
Side 1	1	Building bottom left to right	9.820	9.815	0.0055
	2	Bottom window wall to wall	0.570	0.586	-0.0160
Back	3	Gas valve big	0.600	0.593	0.0067
	4	Gas valve small	0.400	0.370	0.0300
	5	Window bottom vent glass	2.580	2.600	-0.0200
	6	Glass guard Width	0.860	0.822	0.0380
	7	Glass cover length	2.200	2.120	0.0800
	8	Protrusion	0.200	0.215	-0.0150
	9	Window inside	1.130	1.115	0.0150
	10	Window inside	0.560	0.600	-0.0400
Side 2	11	Connecting wall	3.070	3.058	0.0120
	12	Window width wall to wall	0.550	0.578	-0.0280
	13	Floor tile	0.880	0.870	0.0101
	14	Bordure	4.000	4.021	-0.0209
	15	Side wall	2.510	2.501	0.0095
	16	Intermediate door wall to wall	1.000	0.953	0.0474
Front	17	Floor ventilation	9.870	9.907	-0.0369
	18	Main door	2.840	2.838	0.0025
	19	Small marble next to the main door	0.910	0.920	-0.0100
	20	Front wall width	0.320	0.294	0.0257

As a result of statistical analysis, the RMSE of the measurement differences was determined to be 2.95 cm. The StD of the differences was approximately 3 cm. The mean of the measurement differences was 4.8 mm, while the minimum measurement difference value was -4 cm. The maximum measurement difference was 8 cm (Table 4). The graph displaying the statistical analysis results of the measurement differences is presented in Figure 7.

Table 4. Statistical analysis of differences (Min: Measurement Number 10 and Max: Measurement Number 7)

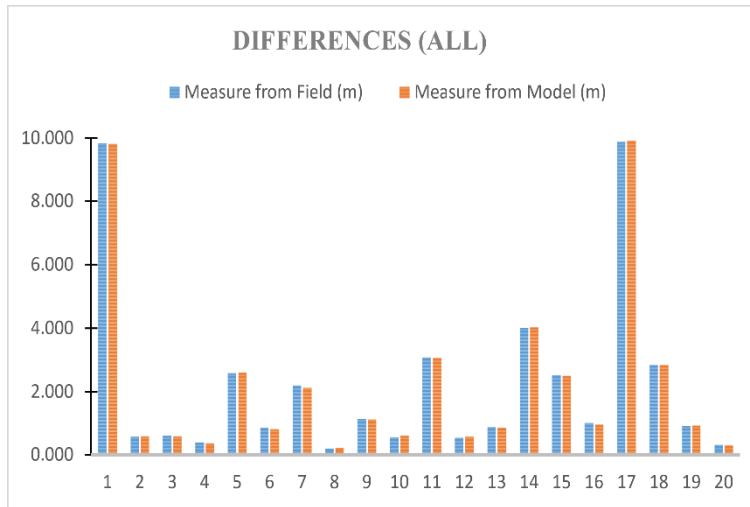| RMSE (m)	StD (m)	Mean (m)	Median (m)	Min. (m)	Max. (m)
0.0295	0.0299	0.0048	0.0061	-0.0400	0.0800

Figure 7. Chart of statistical analysis of differences

Given the normal distribution of error, the accuracy value is calculated within a certain confidence interval. The statistical results calculated at the 95% confidence interval for all the different measures are given in Table 5 and Figure 8 contains the graphical representation of the analysis.

Table 5. Statistical analysis of differences values within the 95% confidence interval

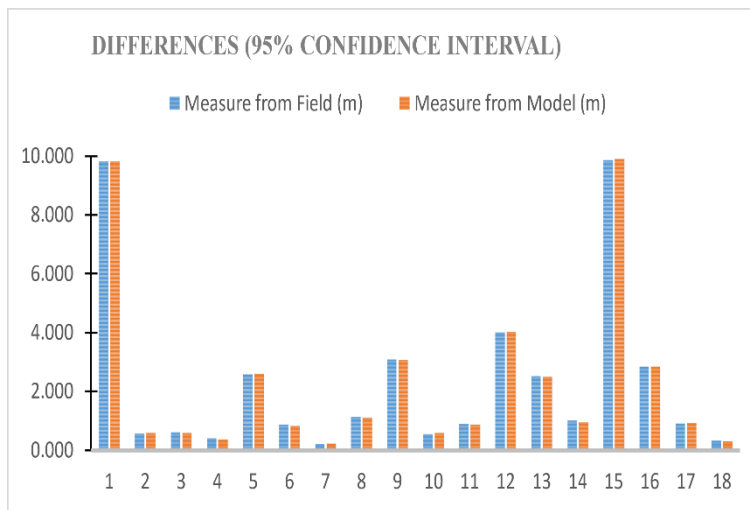| RMSE (m)	StD (m)	Mean (m)	Median (m)	Min. (m)	Max. (m)
0.02292	0.02337	0.00309	0.00610	-0.03690	0.04740

Figure 8. Chart of statistical analysis of differences within the 95% confidence interval

4. CONCLUSIONS

Within the scope of the study, the 3D modeling of Meliha Ercan Guest House, located within the campus of Selçuk University, was carried out using TLS and UAS. In this research, point data (the building's roof and back facade) that cannot be obtained by TLS were attempted to be completed with point data obtained via UAS photogrammetry. It has been revealed with the research that UAV data can be used in cases where the roofs of the buildings cannot be obtained with TLS or that TLS data is suitable for integration in cases where the side facades of the building cannot be modeled with the UAV data. In order to assess the accuracy of the created 3D model, the lengths of the horizontal and vertical facades of the building were determined using the classical measurement technique. The identical facades were

measured on the created model, and statistical analysis of the measurement difference was conducted. As a result, the RMSE of the 3D model obtained at a 95% confidence interval was 2.29 cm, and its StD was 2.34 cm. Therefore, in cases where appropriate image/data acquisition is limited due to unsuitable terrain conditions or incomplete data that cannot be obtained with a single measurement technique, point data obtained from multiple sources were combined, and the applicability of the method as demonstrated by the accuracy of the resulting 3D model. It has been shown in the study that by merging point data from multiple sources, a more accurate and lesser facade 3D model can be obtained as a void. In addition, in analyzing the accuracy of the transformation matrix function used to combine different data types, the 1:1.012 scale reveals an acceptable modeling result.

Declaration of Ethical Standards

The authors declare that be aware and accept all ethical standards.

Credit Authorship Contribution Statement

Lütfiye Karasaka: Visualization, Investigation, Supervision. **Hasan Bilgehan Makineci**: Data Collection, Writing- Reviewing and Editing. **Kasım Erdal**: Software, Validation.

Declaration of Competing Interest

The authors declared that they have no conflict of interest.

Funding / Acknowledgements

Data Availability

The datasets generated and analysed during the current study are not publicly available but are available from the corresponding author on reasonable request.

REFERENCES

[1]   Lichti, D. D., W. Tredoux, R. Maalek, P. Helmholz and R. Radovanovic, "Modelling extreme wide-angle lens cameras." The Photogrammetric Record, 2021.

[2]   Karasaka, L., H. Karabörk, B. Makineci, A. Onurlu and G. İşler, "Indoor Surveying with Terrestral Photogrammetry: A Case Study for Sırçalı Masjid" **6**: 810-817, 2018.

[3]   Beyene, S. M., "Estimation of Forest Variable and Aboveground Biomass using Terrestrial Laser Scanning in the Tropical Rainforest." Journal of the Indian Society of Remote Sensing **48**(6): 853-863, 2020.

[4]   Wang, C., X. Xu, L. Yu, H. Li and J. B. H. Yap, "Grid algorithm for large-scale topographic oblique photogrammetry precision enhancement in vegetation coverage areas." Earth Science Informatics **14**(2): 931-953, 2021.

[5]   Kushwaha, S., K. R. Dayal, S. Raghavendra, H. Pande, P. S. Tiwari, S. Agrawal and S. Srivastava, 3D Digital documentation of a cultural heritage site using terrestrial laser scanner—A case study. Applications of Geomatics in Civil Engineering, Springer**:** 49-58, 2020.

[6]   Shokri, D., H. Rastiveis, W. A. Sarasua, A. Shams and S. Homayouni, "A Robust and Efficient Method for Power Lines Extraction from Mobile LiDAR Point Clouds." PFG–Journal of Photogrammetry, Remote Sensing Geoinformation Science: 1-24, 2021.

[7]   Ulvi, A., "Documentation, Three-Dimensional (3D) Modelling and visualization of cultural heritage by using Unmanned Aerial Vehicle (UAV) photogrammetry and terrestrial laser scanners." International Journal of Remote Sensing **42**(6): 1994-2021, 2021.

[8]   Herban, I. and C. B. Vilceanu, "Terrestrial laser scanning used for 3D modeling. 12th International Multidisciplinary Scientific GeoConference, 2012.

[9]   Arıkan, D., F. Yıldız and H. B. Makineci, "Hava Lidarı Verilerine Uygulanan Farklı Enterpolasyon Yöntemlerinin Sam Doğruluğuna Etkisi, " Konya Mühendislik Bilimleri Dergisi **9**(2): 377-394, 2021

[10]   Deliry, S. I. and U. Avdan, "Accuracy of Unmanned Aerial Systems Photogrammetry and Structure from Motion in Surveying and Mapping: A Review." Journal of the Indian Society of Remote Sensing **49**(8): 1997-2017, 2021

[11]   Dhulkefl, E., A. Durdu and H. Terzioğlu, "DIJKSTRA ALGORITHM USING UAV PATH PLANNING." Konya Mühendislik Bilimleri Dergisi **8**: 92-105, 2020

[12]   Makineci, H. B., H. Karabörk and A. Durdu, "ANN estimation model for photogrammetry-based UAV flight planning optimisation." International Journal of Remote Sensing: 1-23, 2021.

[13]   Wierzbicki, D., "Multi-camera imaging system for UAV photogrammetry." Sensors **18**(8): 2433, 2018.

[14]   Alfio, V. S., D. Costantino and M. Pepe, "Influence of Image TIFF Format and JPEG Compression Level in the Accuracy of the 3D Model and Quality of the Orthophoto in UAV Photogrammetry." Journal of Imaging **6**(5): 30, 2020.

[15]   Toprak, A. S., N. Polat and M. Uysal, "3D modeling of lion tombstones with UAV photogrammetry: a case study in ancient Phrygia (Turkey)." Archaeological Anthropological Sciences **11**(5): 1973-1976, 2019.

[16]   Pepe, M. and D. Costantino, "Uav photogrammetry and 3d modelling of complex architecture for maintenance purposes: The case study of the masonry bridge on the sele river, italy." Periodica Polytechnica Civil Engineering **65**(1): 191-203, 2021.

[17]   Makineci, H. B., H. Karabörk and A. Durdu, "Comparison of Digital Elevation Models Produced with Photogrammetric Usage of UAV by Geodetic Techniques." Türkiye Uzaktan Algılama Dergisi **2**(2): 58-69, 2020.

[18]   Makineci, H. B., and Karasaka, L., "Investigation of 3D models acquired with UAV oblique images". Turkish Journal of Geosciences, 2(2), 13-20, 2021.

[19]   Karabörk, H., L. Karasaka, H. B. Makineci, A. Tanrıverdi, B. Yener, N. Ulutaş and F. N. Öztürk, "3D Modelling of Geometric Triangle Construction Elements in Indoor Spaces: A Case Study for Tahir and Zühre Masjid." International Journal of Environment Geoinformatics **6**(1): 135-138, 2019.

[20]   Šašak, J., M. Gallay, J. Kaňuk, J. Hofierka and J. Minár, "Combined use of terrestrial laser scanning and UAV photogrammetry in mapping alpine terrain." Remote Sensing **11**(18): 2154, 2019.

[21]   Yurtseven, H., "Comparison of GNSS-, TLS-and different altitude UAV-generated datasets on the basis of spatial differences." ISPRS International Journal of Geo-Information **8**(4): 175, 2019.

[22]   Bolkas, D., B. Naberezny and M. Jacobson, "Comparison of sUAS Photogrammetry and TLS for Detecting Changes in Soil Surface Elevations Following Deep Tillage." Journal of Surveying Engineering **147**(2): 04021001, 2021.

[23]   Hirt, P.-R., Y. Xu, L. Hoegner and U. Stilla, "Change Detection of Urban Trees in MLS Point Clouds Using Occupancy Grids." PFG–Journal of Photogrammetry, Remote Sensing Geoinformation Science: 1-18, 2021.

[24]   Achille, C., A. Adami, S. Chiarini, S. Cremonesi, F. Fassi, L. Fregonese and L. Taffurelli, "UAV-based photogrammetry and integrated technologies for architectural applications—methodological strategies for the after-quake survey of vertical structures in Mantua (Italy)." Sensors **15**(7): 15520-15539, 2015.

[25]   Beg, A., Boyutlu Modellemede Yersel Lazer Tarama ve İnsansız Hava Araçları Verilerinin Entegrasyonu ve Kilistra Antik Kenti Örneği Master, Yüksek Lisans Tezi, TC Selçuk Üniversitesi, Fen Bilimleri Enstitüsü, Konya, 2018.

[26]   Jo, Y. H. and S. Hong, "Three-dimensional digital documentation of cultural heritage site based on the convergence of terrestrial laser scanning and unmanned aerial vehicle photogrammetry." ISPRS International Journal of Geo-Information **8**(2): 53, 2019.

[27]   Valenti, R. and E. Paternò, "A comparison between TLS and UAV technologies for historical investigation." Int. Arch. Photogramm. Remote Sens. Spatial Inf. Sci **42**(2): W9, 2019.

[28]   Wijesingha, J., T. Moeckel, F. Hensgen and M. Wachendorf, "Evaluation of 3D point cloud-based models for the prediction of grassland biomass." International Journal of Applied Earth Observation Geoinformation **78**: 352-359, 2019.

[29]   Lussem, U., J. Schellberg and G. Bareth, "Monitoring forage mass with low-cost UAV data: case study at the Rengen grassland experiment." PFG–Journal of Photogrammetry, Remote Sensing Geoinformation Science **88**(5): 407-422, 2020.

[30]   Elkhrachy, I., "Accuracy Assessment of Low-Cost Unmanned Aerial Vehicle (UAV) Photogrammetry." Alexandria Engineering Journal **60**(6): 5579-5590, 2021.

[31]   Jiménez-Jiménez, S. I., W. Ojeda-Bustamante, M. d. J. Marcial-Pablo and J. Enciso, "Digital Terrain Models Generated with Low-Cost UAV Photogrammetry: Methodology and Accuracy." ISPRS International Journal of Geo-Information **10**(5): 285, 2021.

[32]   Xiao, T., X. Wang, F. Deng and C. Heipke, "Sequential Cycle Consistency Inference for Eliminating Incorrect Relative Orientations in Structure from Motion." PFG–Journal of Photogrammetry, Remote Sensing Geoinformation Science: 1-17, 2021.